Environment Canada
Environnement Canada

National Hydrology Research Institute

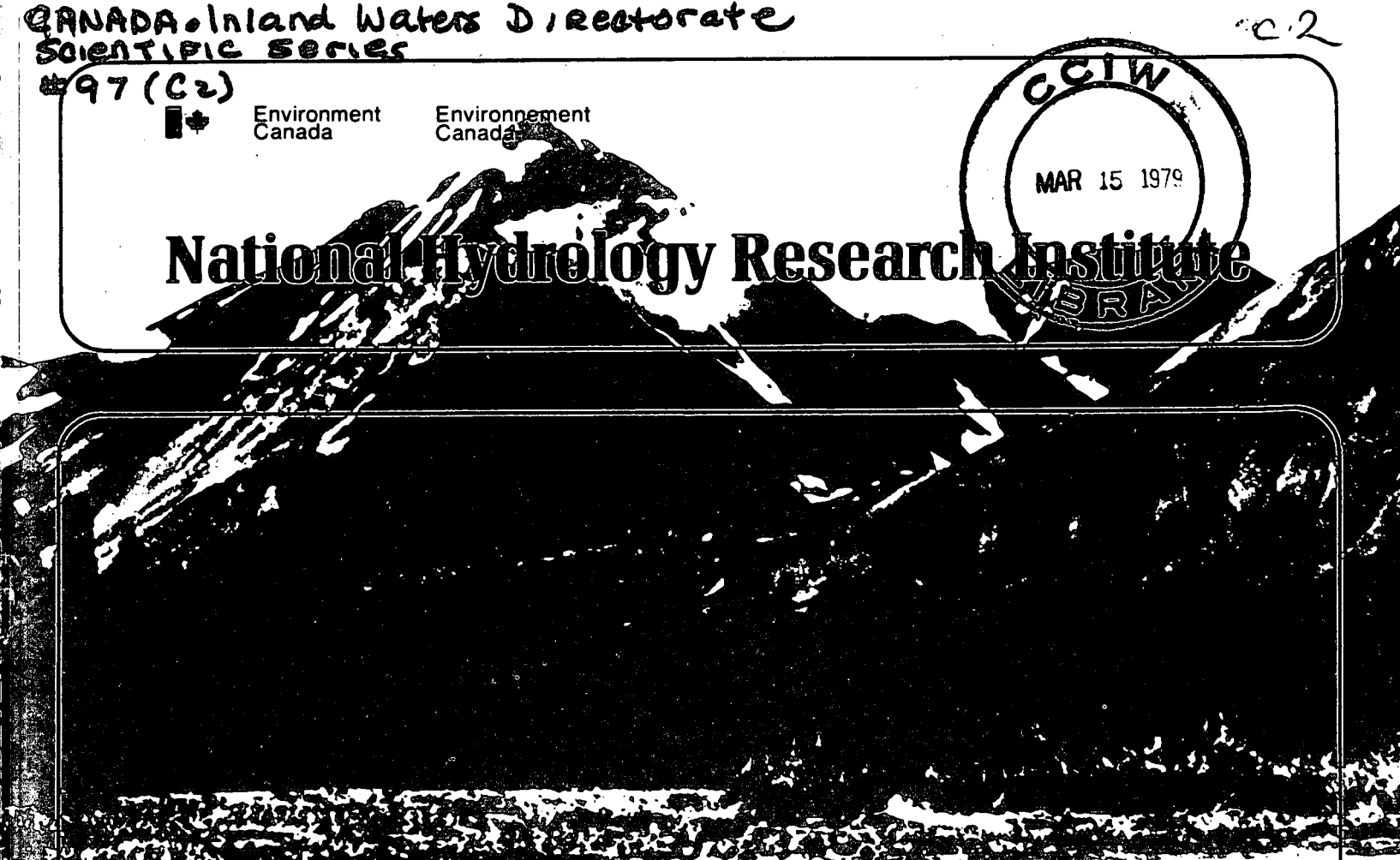

NHRI PAPER NO. 2
IWD SCIENTIFIC SERIES NO. 97

Impact Force of Snow

R. Perla, T. Beck and J. Banner

NHRI

NATIONAL HYDROLOGY RESEARCH INSTITUTE,
INLAND WATERS DIRECTORATE,
OTTAWA, CANADA, 1978

Environment Canada Environnement Canada

National Hydrology Research Institute

NHRI PAPER NO. 2
IWD SCIENTIFIC SERIES NO. 97

Impact Force of Snow

R. Perla, T. Beck and J. Banner

NHRI

NATIONAL HYDROLOGY RESEARCH INSTITUTE,
INLAND WATERS DIRECTORATE,
OTTAWA, CANADA, 1978.

Cat. No. EN36-502/97

ISBN 0-662-10312-2

Contents

	Page
ABSTRACT	v
RÉSUMÉ	v
INTRODUCTION	1
DESCRIPTION OF TESTS	1
RESULTS	3
THEORY OF SNOW IMPACT	6
SUMMARY AND CONCLUSIONS	8
REFERENCE	8

Tables

1. Summary of test results	3
2. Approximate impact on each cell and comparison of peak impact pressure	4

Illustrations

Figure 1. Apparatus used to test impact of snow cylinders	2
Figure 2. Hand tracings of oscillograph wave forms	5
Figure 3. Oscillograph wave form from test No. 36	6
Figure 4. Comparison of impact models	6

Abstract

Cylindrical blocks of snow (mass 20 to 50 kg) were dropped from a height of 10 m onto a circular aluminum plate (thickness 25 mm). Impact forces were measured by load cells and recorded on magnetic tape. For a 50-kg mass, the peak force was 28 kN, occurring about 7 ms after initiation of impact, and decaying to 14 kN in an additional 17 ms. The impact force as a function of time could be represented by

$$F(t) = \frac{4 M V_o^3 t}{d^2} \exp\left(- \frac{2 V_o t}{d}\right)$$

which was derived by assuming that the centre of mass of the sample (mass M) decelerates from an impact speed V_o to rest in a distance d within a force field proportional to sample compression and velocity of compression. The 10-m drop height induced a speed (V_o = 13.5 m/s) that was sufficient to flatten and disaggregate the samples. Prediction of F(t) based on assuming d equal to half the sample height is in agreement with measured values.

Résumé

On a lâché des blocs cylindriques de neige (masse de 20 à 50 kg) d'une hauteur de 10 m, sur une plaque circulaire en aluminium d'une épaisseur de 25 mm. Les forces d'impact ont pu être mesurées au moyen de cellules dynamométriques et enregistrées sur bande magnétique. Pour une masse de 50 kg, la force de pointe était de 28 kN et s'exerçait environ 7 ms après le début de l'impact, diminuant ensuite jusqu'à 14 kN dans les 17 ms suivantes. La force d'impact en fonction du temps pourrait être exprimée par la formule suivante:

$$F(t) = \frac{4 M V_o^3 t}{d^2} \exp\left(- \frac{2 V_o t}{d}\right)$$

laquelle est dérivée en supposant que le centre de la masse de l'échantillon (masse M) décélère d'une vitesse d'impact V_o pour s'arrêter dans une distance d à l'intérieur d'un champs de force proportionnel à la compression de l'échantillon et à la vitesse de compression. La chute d'une hauteur de 10 m a engendré une vitesse (V_o = 13.5 m/s) suffisante pour aplatir et désagréger l'échantillon. La valeur attendue de F(t), en supposant que d est égal à la moitié de la hauteur de l'échantillon, concorde avec les valeurs mesurées.

Impact Force of Snow

R. Perla, T. Beck and J. Banner

INTRODUCTION

If a snow avalanche is modeled as a fluid of density ρ, moving at velocity V, then on the basis of dimensional analysis the impact pressure P should be given by an expression of the form

$$P = k\rho V^2. \quad (1)$$

The value of k depends critically on the details of the model. For example, assuming the fluid to be incompressible and inviscid, then in accordance with Bernoulli's equation, k is 0.5, and P is interpreted as the *stagnation pressure* at the front of the moving avalanche. If we assume the fluid to be compressible, then it can be argued from the conservation of mass and momentum that $k > 1$, and approximately

$$k = (\rho + \Delta\rho)\Delta\rho \quad (2)$$

where $\Delta\rho$ is the increase in snow density after impact (Mellor, 1968).

The fluid model is an attractive simplification; however, anyone who has searched the ruins of an avalanche disaster is aware that avalanches carry lumps of snow in various sizes that depend on the cohesiveness of the snow and the run-out distance of the avalanche. There is little doubt that a significant portion of the destructive impact of the avalanche is transmitted by collisions of discrete masses, rather than as pressure of a continuous fluid. A model founded on the fluid hypothesis may only be valid where the collision area is large compared with the size of the discrete snow masses.

We initially attempted to measure discrete avalanche forces on stands erected above a highway shed at Rogers Pass, B.C., in cooperation with related research conducted by the Division of Building Research (National Research Council). After 2 years of disappointing results, mostly due to equipment failures, but in part due to our inability to interpret pressure measurements produced by small targets (area 1 to 10 cm^2), we decided to retreat to a more controllable experiment using large target areas.

The purposes of this report are to present the results of our experiments, and to discuss these results in terms of theoretical models of snow impact. The work was done at our snow avalanche laboratory (Sunshine, Alberta) in cooperation with Parks Canada. Snow samples were taken from an adjacent avalanche study plot erected and maintained by the Warden Service, Banff National Park.

DESCRIPTION OF TESTS

Our tests involved lifting a cylindrical bucket filled with snow to a height of approximately 10 m, and then dropping the snow onto a circular target supported by four load cells (see Fig. 1). Deflection of the load cells produced four voltage signals, which were amplified and recorded on a four-channel magnetic tape recorder.

To obtain a cohesive cylinder of snow, we inserted the bucket carefully into the snow pack, but it was not possible to collect a sample of constant density. From top to bottom of cylinder, the density varied by 100% or more. In a few cases, we deliberately packed snow in the bucket to obtain higher densities than available naturally. The bottom of the bucket was a four-segment trapdoor, which we unlatched manually (by climbing the pole).

We raised by winch a total of 37 snow cylinders to the drop-height position. In six cases, the snow cylinders either: (a) failed to release from the bucket as a cohesive unit as a result of sticking to the sides of the bucket; or (b) were deflected by the trapdoors and completely missed the target. In one test, we forgot to energize the amplifier. The remaining 30 tests were divided between "apparent bull's-eyes" and obvious off-centre impacts. In a few cases the snow cylinder was deflected slightly by the trapdoors and hit the target in a tilted rather than a flat orientation. However, in most cases, the impact appeared to be flat. The above experimental mishaps produced a wide scatter of results that are more fully explained later in this paper.

The velocity V_0 at initiation of impact was computed to be 13.5 m/s based on an actual drop height of 9.71 m, an air-drag coefficient C_D equal to unity, and a sample mass of 40 kg. The air-drag correction is small in this experiment (V_0 in a vacuum would be 13.8 m/s).

The dynamic response of the measuring system is an important consideration in any impact test. We optimized

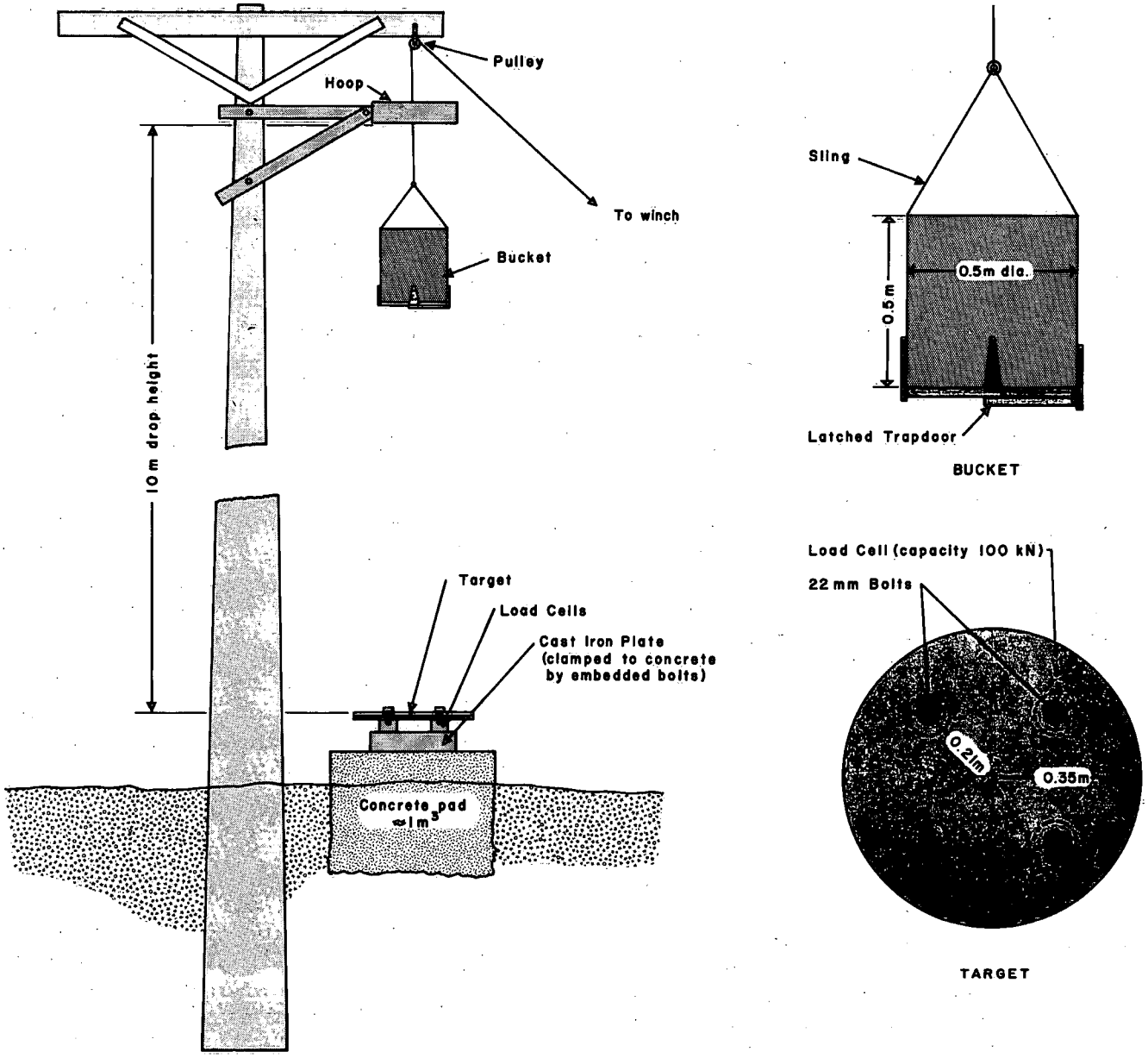

Figure 1. Snow cylinders were lifted in a bucket to a drop height of approximately 10 m. The snow was released through a trapdoor in the bucket. Impact on target was measured with four load cells. Dimensions shown in figure are rough approximations, and not to scale.

response speeds by using stiff load-cells, and a thick, light-weight target. The latter was a 25-mm-thick aluminum plate with a mass M_P = 26.8 kg. To test response speed, we hit the target with a steel sledge hammer and noted a natural frequency $f_N \cong 3000$ Hz. As a cross check, we computed total system stiffness K_T from

$$f_N = (1/2\pi)\sqrt{K_T/M_p} \qquad (3)$$

and found $K_T = 9.5 \times 10^9$ N/m. Since the nominal stiffness of four load cells in parallel[1] is $K_L \cong 1.75 \times 10^{10}$, it appears that approximately one-half of the system deflection is due to the load cells, and the other half due to the deflection of the target plate and mounting hardware. The above measurement (3000 Hz) and computed K values seem self-consistent.

[1] Capacity of each load cell is approximately 110 kN. Full-load capacity of four cells in parallel is therefore 440 kN. Deflection at full load is approximately 0.025 mm.

As it turned out, the rise time of our 30 impacts was never greater than 5 ms, or in terms of frequency, never over 50 Hz. The system was therefore sufficiently fast by a wide margin. For a load-cell displacement of magnitude L, the inertial correction ($\cong M_P L$) amounts to less than 1% of the load-cell output ($\cong K_L L$). Furthermore, even if K_T was two orders of magnitude smaller ($K_T \cong 10^8$ N/m), f_N would still be sufficiently high ($f_N \cong 400$ Hz) for accurate impact measurements with inertial errors of a few percent maximum.

RESULTS

Data describing our 37 attempts to measure snow impact are given in Table 1, which also provides a column of notes explaining some of our experimental problems. A "bull's eye" consisted of flattening and disaggregation of the cylindrical sample (diameter 0.5 m) within the target area (diameter 0.7 m). Although fragments flew in various directions, it appeared that most of the snow mass collapsed within the target area (and had to be cleaned off the target at the conclusion of the test).

Sample densities shown in Table 1 are based on the sample volume (8.133×10^{-2} m^3) and on measurements of sample mass M, which ranged from 20.5 to 53.5 kg. Snow temperature was measured at the centre of the sample, and beginning with test No. 26, was 0°C with increasing amounts of free water developing through the month of May. This water provided a lubricating film on the paraffined interior of the aluminum bucket, permitting the sample to slide from the bucket more smoothly compared with the earlier tests (Nos. 1-25) with dry, colder snow. The improvement of targeting in test Nos. 26 to 37 was also due to modifying the latch mechanism to open the trapdoors faster; this minimized lateral deflection of the sample.

Visual observation of impact determined if a test could be subjectively classified as *apparent bull's-eye,*

Table 1. Summary of Test Results

Test No.	Date 1977	Sample density (kg/m^3)	Sample temp. (° C)	Peak force (kN)	Time to peak (ms)	M V_o (Ns)	$\int$Fdt (Ns)	Notes
1	15 March	291	-5.0	9.52	14.7	320	238	Slightly off-centre
2	17 March	257	-4.5	8.16	14.7	282	211	Slightly off-centre
3	17 March	–	–	–	–	–	–	Forgot to energize amplifier
4	17 March	252	-5.0	7.72	6.88	277	223	Slightly off-centre
5	17 March	286	-4.0	6.80	10.6	315	194	Missed 1/4 of target
6	18 March	–	–	–	–	–	–	Missed completely
7	18 March	–	–	–	–	–	–	Snow stuck in bucket
8	18 March	277	-2.5	8.84	6.89	304	231	Slightly off-centre
9	21 March	264	-5.0	5.88	10.0	290	122	Missed 1/4 of target
10	21 March	314	-4.0	8.40	7.50	344	164	Missed 1/2 of target
11	21 March	338	-3.0	10.6	11.9	371	285	Apparent bull's-eye
12	22 March	–	–	–	–	–	–	Snow released in 2 pieces
13	22 March	283	-3.5	5.00	13.8	311	116	Missed 1/4 of target
14	22 March	277	-3.5	9.28	9.06	304	225	Slightly off-centre
15	22 March	274	-3.5	4.52	15.0	301	126	Missed 1/2 of target
16	24 March	–	–	–	–	–	–	Snow stuck in bucket
17	24 March	295	-2.5	7.24	14.4	324	176	Missed 1/4 of target
18	24 March	301	-2.0	9.08	6.88	331	218	Missed 1/4 of target
19	24 March	293	-2.5	10.2	6.25	321	248	Apparent bull's-eye
20	12 April	–	–	–	–	–	–	Snow released in 2 pieces
21	12 April	307	-0.5	9.52	16.9	338	235	Apparent bull's-eye, but tilted
22	12 April	314	-0.5	13.6	11.9	344	326	Slightly off-centre
23	12 April	307	-0.5	5.44	21.9	338	125	Missed 3/4 of target
24	12 April	314	-0.5	11.1	10.3	344	241	Slightly off-centre
25	12 April	–	–	–	–	–	–	Snow released in 2 pieces
26	3 May	430	Damp	17.7	7.50	473	388	Apparent bull's-eye
27	3 May	492	Damp	16.3	5.00	540	464	Apparent bull's-eye
28	3 May	584	Damp	24.7	6.88	641	523	Apparent bull's-eye
29	12 May	658	Wet	20.9	8.13	722	661	Slightly off-centre
30	12 May	621	Wet	20.0	5.63	682	612	Apparent bull's-eye
31	12 May	621	Wet	28.4	8.13	682	795	Apparent bull's-eye
32	16 May	541	Wet	22.2	6.88	594	478	Slightly off-centre
33	16 May	504	Wet	17.2	8.75	554	428	Slightly off-centre
34	16 May	566	Wet	26.3	7.81	621	532	Apparent bull's-eye
35	20 May	436	Wet	17.2	8.44	479	393	Apparent bull's-eye
36	20 May	418	Wet	17.2	7.50	459	369	Slightly off-centre
37	20 May	424	Wet	16.3	7.50	466	400	Apparent bull's-eye

slightly off-centre, 1/4 miss, 1/2 miss, 3/4 miss, or complete miss. There was good agreement between this subjective classification and quantitative analysis of the balance of the four load-cell signals. For example, in tests subjectively classified as 1/2 miss, two load cells produced strong positive signals, and the other two cells produced either weak positive signals or in some instances a negative signal, indicating tension. The signal balance was closer for tests classified as apparent bull's-eye, although there was always large variation among the individual signals (see Table 2).

The four load-cell signals were added algebraically and transcribed on an oscillograph. Hand-traced sketches of the oscillograph recordings are shown in Figure 2. The band of experimental noise (not shown in Figure 2) was typically about 1.8 kN wide (see Fig. 3).

As shown in Figures 2 and 3, the impact wave form consisted of a fast rise to peak value followed by a slower decay to a small residual value, which represents the static load of the sample on the target. The time to peak (t_{max}) varied from 5 to 16.9 ms. If the impact frequency is defined as $(4\ t_{max})^{-1}$, then the corresponding frequency range is 50 to 15 Hz. The lower values of t_{max} (higher frequency) tend to correlate (but not completely) with bull's-eyes.

Table 1 compares momentum sent to the target, MV_o, and the momentum measured by the load cells (the area $\int F dt$ of the oscillograph trace). It appears possible to account for most of the momentum, especially if a "target miss" is considered as a loss of momentum. In those tests where most of the momentum can be accounted for, we believe we have correctly measured the impact force of our samples. In particular, we feel that our final tests, Nos. 26-37, represent a fairly good set of measurements in terms of momentum balance as well as visual observations of target accuracy. Although these samples contained ap-

Table 2. Approximate Impact on each Cell as Read on Portable Storage Oscilloscope during Field Tests (100 mV = 1.1 kN). Comparison of peak impact pressure ($P_{max} = F_{max}/A$) and ρV_o^2. $A = 0.173\ m^2$, $V_o = 13.5$ m/s, ρ and F_{max} from Table 1

Test No.	Approximate impact (kN)				Notes (from Table 1)	F_{max} (kN)	F_{max}/A (kN/m²)	ρV_o^2 (kN/m²)
	Cell 1	Cell 2	Cell 3	Cell 4				
1	1.1	5.0	1.8	1.4	Slightly off-centre	9.52	55	53
2	2.3	1.8	0.8	3.4	Slightly off-centre	8.16	47	47
3	–	–	–	–	Forgot to energize amplifier	–	–	–
4	2.6	1.5	0.6	3.9	Slightly off-centre	7.72	45	46
5	0.0	2.6	3.2	2.8	Missed 1/4 of target	6.80	39	52
6	–	–	–	–	Missed completely	–	–	–
7	–	–	–	–	Snow stuck in bucket	–	–	–
8	1.1	3.6	1.1	1.0	Slightly off-centre	8.84	51	51
9	-2.3	1.6	2.8	2.3	Missed 1/4 of target	5.88	34	48
10	4.8	2.8	0.0	0.0	Missed 1/2 of target	8.40	49	57
11	1.4	1.9	1.2	5.9	Apparent bull's-eye	10.6	61	62
12	–	–	–	–	Snow released in 2 pieces	–	–	–
13	-1.7	0.9	1.6	4.0	Missed 1/4 of target	5.00	29	52
14	1.4	1.1	0.5	5.9	Slightly off-centre	9.28	54	51
15	-2.0	1.1	2.3	2.9	Missed 1/2 of target	4.52	26	50
16	–	–	–	–	Snow stuck in bucket	–	–	–
17	-1.1	3.3	3.4	2.3	Missed 1/4 of target	7.24	42	54
18	0.5	3.1	1.9	4.3	Missed 1/4 of target	9.08	53	55
19	2.3	4.0	1.1	3.4	Apparent bull's-eye	10.2	59	53
20	–	–	–	–	Snow released in 2 pieces	–	–	–
21	1.1	2.8	1.4	3.7	Apparent bull's-eye, but tilted	9.52	55	56
22	1.7	1.7	0.5	9.5	Slightly off-centre	13.6	79	57
23	0.2	0.0	0.0	4.5	Missed 3/4 of target	5.44	31	56
24	-1.1	5.2	3.2	2.9	Slightly off-centre	11.1	64	57
25	–	–	–	–	Snow released in 2 pieces	–	–	–
26	2.3	8.2	5.0	2.7	Apparent bull's-eye	17.7	102	78
27	3.9	4.5	2.7	5.7	Apparent bull's-eye	16.3	94	90
28	1.8	7.0	5.0	10.2	Apparent bull's-eye	24.7	143	106
29	4.1	11.3	3.2	1.1	Slightly off-centre	20.9	121	120
30	2.7	4.5	7.3	3.4	Apparent bull's-eye	20.0	116	113
31	10.2	2.3	3.4	10.4	Apparent bull's-eye	28.4	164	113
32	1.7	8.2	9.5	1.4	Slightly off-centre	22.2	128	99
33	3.2	7.3	4.5	0.6	Slightly off-centre	17.2	99	92
34	5.2	3.1	7.9	9.1	Apparent bull's-eye	26.3	152	103
35	7.3	5.9	1.7	1.4	Apparent bull's-eye	17.2	99	80
36	1.1	0.6	5.2	9.1	Slightly off-centre	17.2	99	76
37	2.3	3.4	6.1	2.8	Apparent bull's-eye	16.3	94	77

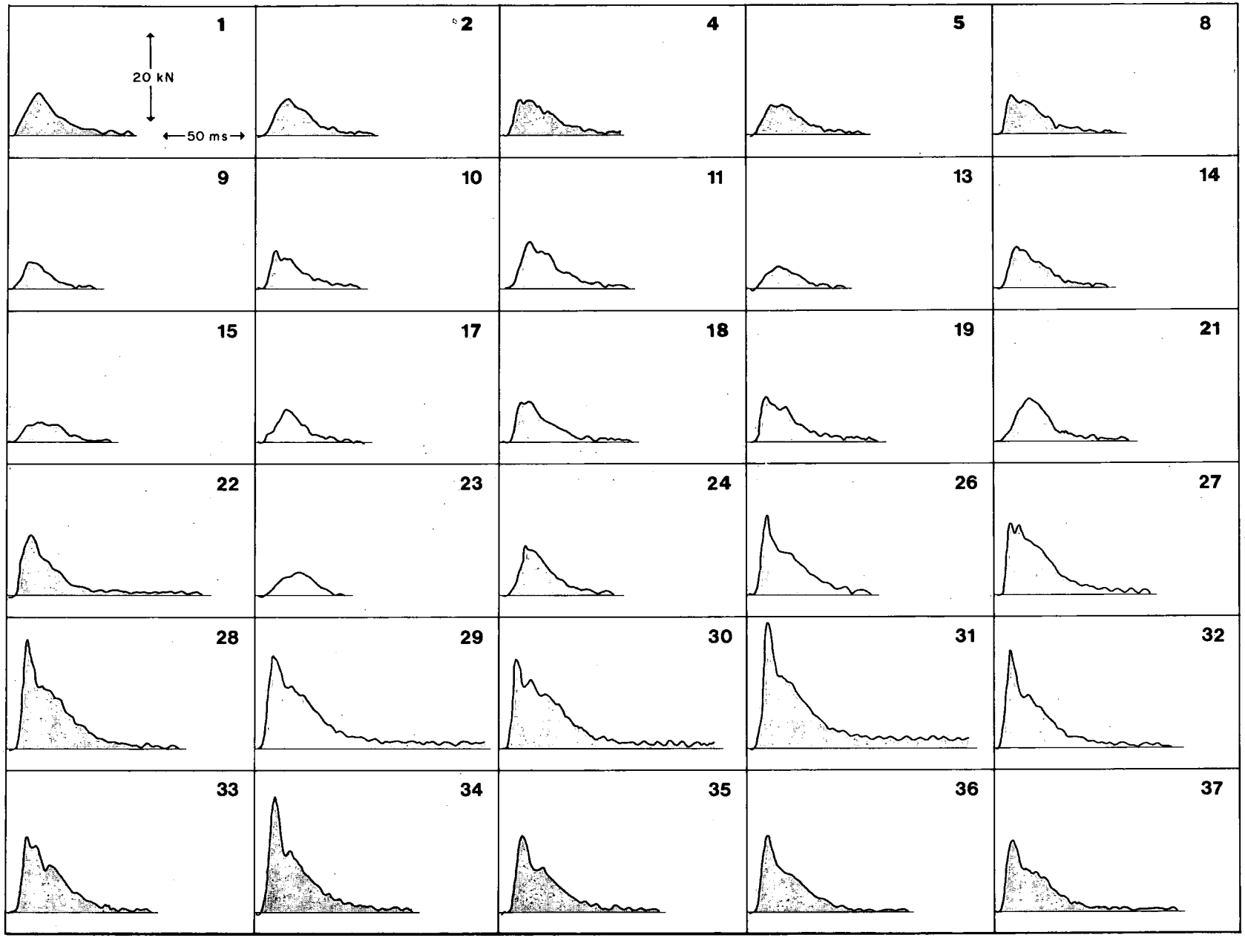

Figure 2. Hand tracings of oscillograph wave forms. Experimental noise is not shown. Tests 3, 6, 7, 12, 16, 20, and 25 were void.

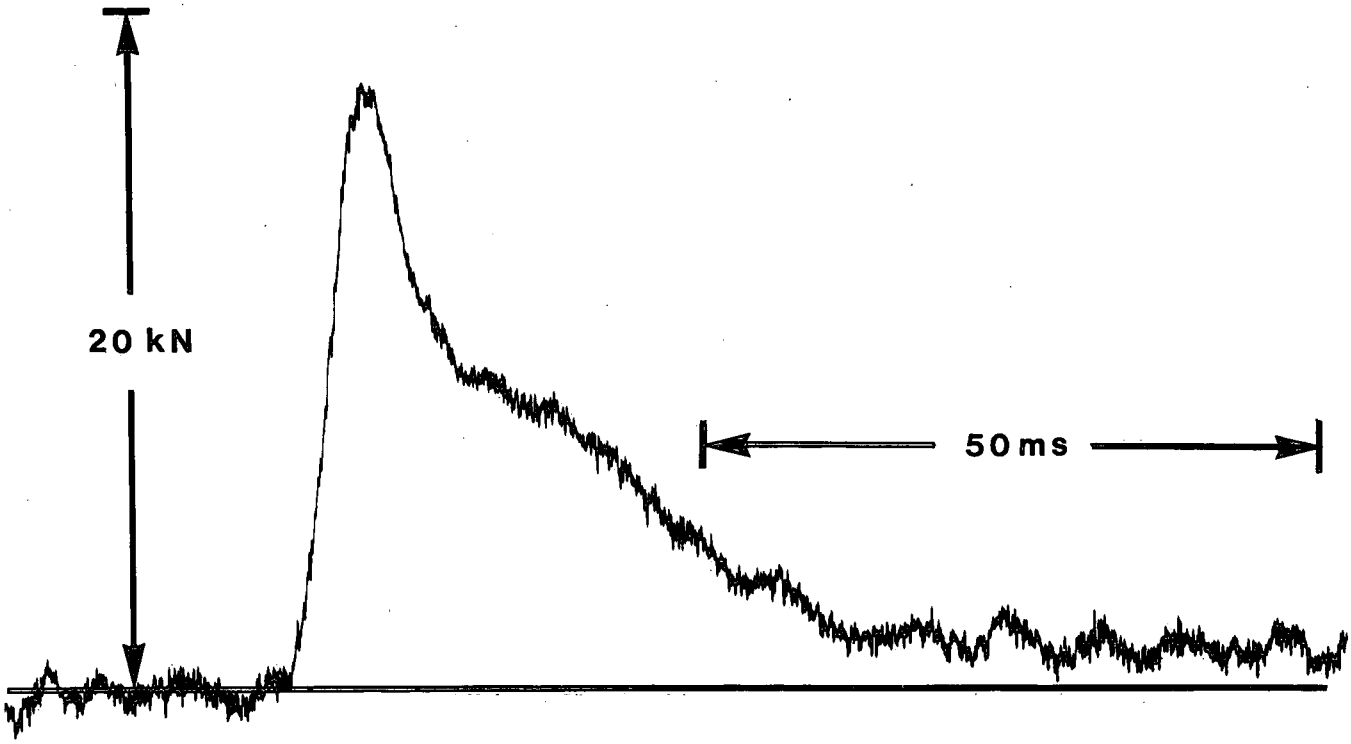

Figure 3. Oscillograph wave form from test No. 36.

preciable amounts of free water, comparisons with the successful tests using dry snow suggest that free water is not an important *independent* variable.

THEORY OF SNOW IMPACT

When a snow mass moving at high speeds strikes a rigid object, the mass disaggregates and flattens considerably. In the case of our snow cylinders, height h = 0.5 m, it was observed that the disaggregated sample flattened to about 0.05 m, or 0.1 h. Although snow fragments move complexly in all directions, it is convenient to imagine the *centre of mass* of the snow sample decelerating from the initial impact speed V_o to standstill in a distance d. At speeds comparable to and greater than those developed in our tests ($V_o \geqslant 13.5$ m/s), d approaches h/2.

It is instructive to consider first a model wherein the centre of mass decelerates with a *constant* value. For this case, the impact force F also has a constant value, given by Newton's Second Law as

$$F = MV_o^2/2d. \qquad (4)$$

This simple model is physically impossible since it implies that F(t) is a step function (see Fig. 4, function A). In any real impact, F(t) varies as a single-valued function from 0 to a peak in a finite time interval.

Let us then consider a slightly more complex model wherein the force (and hence the deceleration) is a sinusoidal function (Fig. 4, function B).

$$F(t) = F_{max} \sin \omega t \qquad (5)$$

Applying the following boundary conditions on the dis-

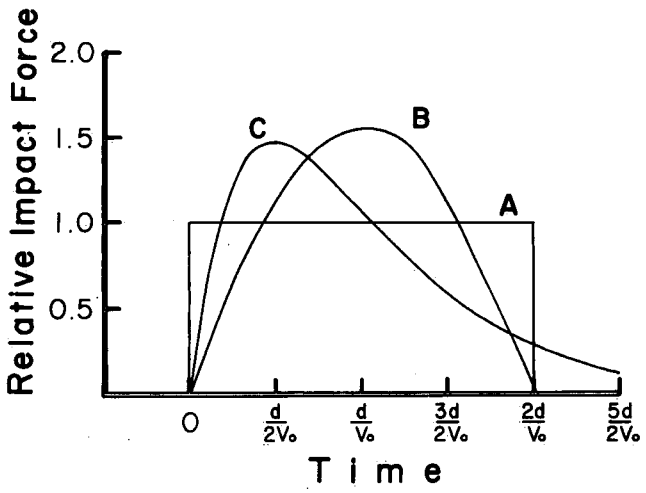

Figure 4. Comparison of impact models: (A) step model, (B) sinusoidal model, (C) exponential model. The time scale is expressed in terms of V_o, the initial impact speed; and d, the displacement of the centre of mass of the sample at the termination of impact.

placement x, the velocity $\dot{x}$ and the deceleration $\ddot{x}$ of the centre of mass

$$\begin{aligned} &\text{at } t = o\text{: } x = o,\ \dot{x} = V_o,\ \ddot{x} = 0 \\ &\text{at } \omega t = \pi\text{: } x = d,\ \dot{x} = 0,\ \ddot{x} = 0 \end{aligned} \tag{6}$$

allows F(t) to be determined as

$$F(t) = \frac{M\pi V_o^2}{4d} \sin \frac{V_o \pi t}{2d} . \tag{7}$$

The choice of a sine function is mathematically convenient, but quite arbitrary. It is possible to choose an alternate function that better describes the characteristic wave forms (Fig. 2), and, moreover, that arises naturally from a consideration of the impact mechanics in the following way. As the sample compresses against the target there is an increasing amount of force, somewhat analogous to the compression of a spring. The force reaches a peak and then decays, analogous to a spring relaxing into a dashpot. The combined analogy is to picture the motion of the centre of mass controlled by a force proportional to displacement and a force proportional to velocity. This analogy is given by Newton's Second Law as

$$M\ddot{x} = a_o x + a_1 \dot{x} \tag{8}$$

where the weight of the sample Mg is assumed to be small in comparison with the deceleration forces.[2] Equation 8 has three possible solutions:

$$x = (A \cos qt + B \sin qt)\, e^{-rt} \tag{9}$$

$$x = (A + Bt)\, e^{-rt} \tag{10}$$

$$x = A e^{-rt} + B e^{-st} \tag{11}$$

Since the oscillatory motion of the centre of mass is negligible compared with its main displacement, solution 9 is rejected. Either (10) or (11) is physically plausible. Either will generate wave forms similar in shape to those shown in Figure 2. Moreover, either will satisfy the required boundary conditions

$$\begin{aligned} &\text{at } t = o\text{: } x = o,\ \dot{x} = V_o,\ \ddot{x} = o \\ &\text{at } t = \infty\text{: } x = d,\ \dot{x} = o,\ \ddot{x} = o \end{aligned} \tag{12}$$

However, to apply solution 11 it is necessary to determine four constants $\{A, B, r, s\}$. It can be shown that it is impossible to determine more than three constants using (12).

The three constants $\{A, B, r\}$ required to complete solution 10 are completely determined from (12) without further assumptions. We therefore choose (10) because of its simplicity, recognizing that (11) is a more refined solution with the potential of a better fit.

From solution 10 the impact force is

$$F(t) = \frac{4 M V_o^3 t}{d^2} \exp\left(-\frac{2V_o t}{d}\right) . \tag{13}$$

The peak force is

$$F_{max} \approx 0.736\ (MV_o^2/d) \tag{14}$$

occurring at

$$t_{max} = d/2V_o \tag{15}$$

after initiation of impact (see Fig. 4, function C).

It is possible to compare predictions of the models summarized in Figure 4: step model (A), sinusoidal model (B), and exponential model (C). Substituting V_o = 13.5 m/s and d = 0.25 m into expressions 4, 7, and 14, we find that the models predict peak force values as follows:

$$\begin{aligned} F_{max} &= 365\ M \\ F_{max} &= 573\ M \\ F_{max} &= 536\ M \end{aligned} \tag{16}$$

If we average results from our best sequence of tests, Nos. 26-37, we obtain $\bar{F}_{max}$ = 20.4 kN for the average sample mass, $\bar{M}$ = 42.7 kg. Substituting M = 42.7 into the set of expressions (16), we obtain the values of F_{max} predicted by the respective models as 15.6, 24.5, and 22.9 kN. The exponential model appears to out-predict its competitors.

More striking is comparison of the tested and predicted values of t_{max}. For tests 26 to 37, the average of t_{max} is 7.3 ms (from Table 1). The respective values predicted by the step, sinusoidal, and exponential models are 0, 18.5, and 9.3 ms. Again, the exponential model gives the best prediction.

A third basis of comparison is the time for the impact force to decay from F_{max} to 1/2 F_{max}. The average for tests 26 to 37 is 16.5 ms. The exponential model again out-predicts the sinusoidal model (15.7 ms compared with

[2] In our tests, the sample weight Mg is about an order of magnitude less than the deceleration forces. Mg can be added as a correction to the solutions of Equation 8.

12 ms). Note that this measure is ambiguous in the step model ($F(t) = 0$ at $t = 0$ and at $t = 37$ ms).

Would the exponential model work as well if the test samples were spheres rather than cylinders? It is more difficult to fabricate snow spheres, and without experimental data it is premature to speculate in detail. We feel that F_{max} would not change drastically for two reasons. First, although there is an obviously great difference in the initial shape of a sphere and cylinder, the initial shapes are soon lost through compression and disaggregation. In both cases, the final shape is a flattened, disaggregated mass. Second, there is less than 10% difference in F_{max} predicted by the sinusoidal and exponential functions, so there is no reason to expect that alternate representations of $F(t)$ satisfying the boundary conditions (12), yield a major change in F_{max}. On the other hand, there is a substantial difference in t_{max} as predicted by the sinusoidal and exponential representations, and we feel less confident that t_{max} will not change significantly for a spherical sample, which could conceivably impact more sinusoidally.

If the values of F_{max} given by Equations 4, 7, and 14 are divided by the collision area that the specimen projects on the target (in our case, the circular base of the cylinder), and if we assume $d = h/2$, and further, if in place of mass/volume we substitute sample density ρ, then we obtain expressions for the maximum impact pressure:

$$\begin{aligned} \text{Step model:} \quad & P_{max} = \rho V_o^2 \\ \text{sinusoidal model:} \quad & P_{max} = (\pi/2)\,\rho V_o^2 \\ \text{exponential model:} \quad & P_{max} = (4/e)\rho V_o^2 \end{aligned} \qquad (17)$$

In Table 2, values of ρV_o^2 are compared with the measured values F_{max}/A, where A is the cylinder area (0.173 m^2). An inspection of tests 26 to 37 indicates that application of Equation 1 to our experiment requires that the value of k exceed unity. However, in an avalanche, individual impacts would be distributed in space and time, and the effective value of k would be lower than the k associated with an individual impact.

SUMMARY AND CONCLUSIONS

A model based on the deceleration of the centre of mass of a snow sample predicts that the impact force of the sample is

$$F(t) = \frac{4MV_o^3 t}{d^2} \exp\left(-\frac{2V_o t}{d}\right)$$

where M is the mass of the sample, V_o is the speed at impact, and d is the distance in which the centre of mass decelerates from V_o to rest. The peak force is

$$F_{max} \approx 0.736\,(M V_o^2/d)$$

and occurs at time

$$t_{max} = d/2V_o .$$

The model was tested on snow cylinders (mass 20 to 50 kg, diameter 0.5 m, height 0.5 m) moving at a speed 13.5 m/s. In these tests, d approached one-half the sample height. Averaging our more reliable test results indicated that a mass of 42.7 kg produces a peak impact force of 20.4 kN in a rise time $t_{max} = 7.3$ ms. The force decayed to 10.2 kN in an additional 16.5 ms. The corresponding predicted values were within 10 to 20% of these experimental averages.

Although no claim is made that our results can be confidently extrapolated to much higher speeds without further experiments, it can be assumed that the higher the speed the closer d approaches one-half the sample height. Thus, it is unlikely that the developed theory fails if V_o increases to the clocked speeds of fast moving avalanches (25 to 50 m/s).

REFERENCE

Mellor, M., 1968. Avalanches. U.S. Army Corps Eng. Cold Reg. Res. Eng. Lab. III-A3. 223 p.